A UNIFIED MODEL OF SOLAR FLARI

KAZUNARI SHIBATA
National Astronomical Observatory
Mitaka, Tokyo 181, Japan

Abstract: A unified model of flares, which we call the *plasmoid-induced-reconnection model*, is presented. This model explains various observed features (e.g., homologous flares, time scale, energy release rate) of impulsive flares, LDE flares, giant arcades associated with filament eruptions or CMEs, and microflares in a unified scheme. This model is an extention (a unified version) of the CSHKP model and the emerging flux model.

1. Introduction

Before *Yohkoh*, solar observers had long thought that solar flares could be classified into two types, such as LDE flares vs impulsive flares, or eruptive vs confined, or two ribbon vs simple loop (or compact), etc. (e.g., Priest 1982). The former has often been thought to be explained by the so called "CSHKP" (Carmichael-Sturrock-Hirayama-Kopp-Pneuman) reconnection model, whereas the latter has been attributed to different models, such as the emerging flux reconnection model (Heyvaerts et al. 1974).

Yohkoh, however, has revealed that there are many common features in both types of flares, e.g., the ejection of hot plasmas (possibly plasmoids) (Shibata et al. 1995, Shibata 1996, Tsuneta 1997, Ohyama and Shibata 1997a,b), x-type or y-type morphology suggesting the presence of current sheets or neutral points (Tsuneta et al. 1992a,b, Masuda et al. 1994, 1995, Tsuneta 1996, 1997), change of field configuration, etc. Even microflares have sometimes shown hot plasma ejections or jets (Shibata et al. 1992b, Shimojo et al. 1996) and change of morphology (possibly as a result of reconnection) (Shibata et al. 1994). It is now not easy to classify flares into two types, and a unified view of flares has emerged on the basis of *Yohkoh* observations (Shibata 1996, 1997, Kosugi and Shibata 1997). This view is also consistent with the statistical properties of many solar flares, such as

T. Watanabe et al. (eds.), Observational Plasma Astrophysics: Five Years of Yohkoh and Beyond, 187–196.

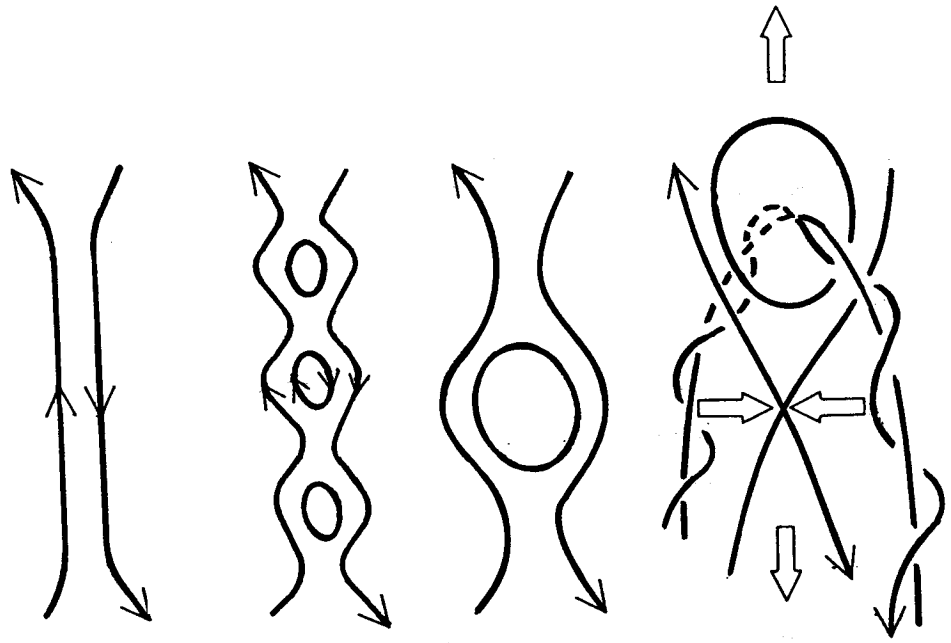

Figure 1. Schematic drawings showing current sheet formation, tearing, coalescence, plasmoid ejection, and triggered fast reconnection at high magnetic Reynolds number, all of which have been found in numerical simulations. In three-dimensional space, the plasmoid would be seen as a helically twisted loop or filament. Eruptive prominences observed in Hα are a kind of plasmoid ejection.

the frequency distribution of flares as a function of X-ray intensity (or flare energy), which shows the same power-law distribution not only for major flares but also for microflares (e.g., Shimizu 1995), and the relationship between the temperature and the emission measure for major and micro flares (e.g., Watanabe 1994).

On the other hand, recent numerical simulations of magnetic reconnection with high spatial resolution have revealed that there are common fundamental (evolutionary) features in fast reconnection at high magnetic Reynolds number ($R_m > 10^3$); once a current sheet is formed, magnetic reconnection proceeds intermittently with nonsteady processes (see Fig. 1), such as tearing in the current sheet, coalescence of magnetic islands (plasmoids), and ejection of plasmoids (e.g., Lee and Fu 1986, Ugai 1989, Shibata et al. 1992a, Yokoyama and Shibata 1994, Karpen et al. 1995, Kusano et al. 1995, Kitabata et al. 1996). It has been found that even reconnection driven by emerging flux (i.e., the emerging flux model) results in the ejection of plasmoids (Shibata et al. 1992a, Yokoyama and Shibata 1994, 1995, 1996) similar to those seen in CSHKP-type reconnection (e.g., Magara et al. 1996, Yokoyama and Shibata 1997). In this sense, there is no fundamental difference in the physics of reconnection in the emerging flux model and in the CSHKP model. These numerical simulation results (see Yokoyama

1997 for a review), especially the common occurrence of plasmoid ejections and associated intermittent nonsteady (bursty) reconnection at high magnetic Reynolds number, are quite similar to actually observed behavior of solar flares as discussed above. Since the magnetic Reynolds number in the active region corona is enormously high $\sim 10^{13}$, it is natural to think that the observed impulsive nature and plasmoid ejections are a consequence of fast reconnection at high magnetic Reynolds number (Shibata 1997).

In this paper, taking account of these recent developements in both observations and numerical simulations, we propose a unified model of solar flares, which we call the *plasmoid-induced-reconnection model* since plasmoid ejections play a key role in triggering fast reconnection in the model. This model unifies not only LDE flares and impulsive flares, but also microflares. In a previous paper (Shibata 1996), we call the former unification the "unified model", and the latter the "grand unified model". However, in this paper, we simply use the term "unified model," since it has become clear that there is no essential difference in our previously defined unified and grand unified models.

2. The Plasmoid-Induced-Reconnection Model

2.1. BASIC FEATURES OF THE MODEL

Observations show that strong acceleration of plasmoids occurs just before the peak of the impulsive phase of flares (Ohyama and Shibata 1997a,b). If the intensity of hard X-rays is a measure of the electric field (i.e., reconnection rate) at the X-point, this suggests that the ejection of high speed plasmoids induces fast inflow, i.e., fast reconnection. Similar behavior has also been found in numerical simulations of reconnection (e.g., Ugai 1989, Yokoyama and Shibata 1994, 1996, Magara et al. 1997).

Hence we adopt the hypothesis that *impulsive energy release due to fast reconnection is induced by the fast ejection of plasmoids.* In this case, the velocity of inflow into the X-point is estimated to be

$$V_{inflow} \sim V_{plasmoid} \sim 50 - 400 \text{ km/s}, \tag{1}$$

from the conservation of mass, assuming that plasma density does not change much during the process. Then, the Alfven Mach number of the inflow becomes

$$M_A = V_{inflow}/V_A \sim 0.02 - 0.1 V_A. \tag{2}$$

This is comparable to the inflow speed expected from Petschek theory. We call this the *plasmoid-induced-reconnection model* (see Fig. 2).

The merit of this model is that it can easily explain *homologous flares*, as illustrated in Figure 3. In either the long current sheet case (e.g., Kitabata

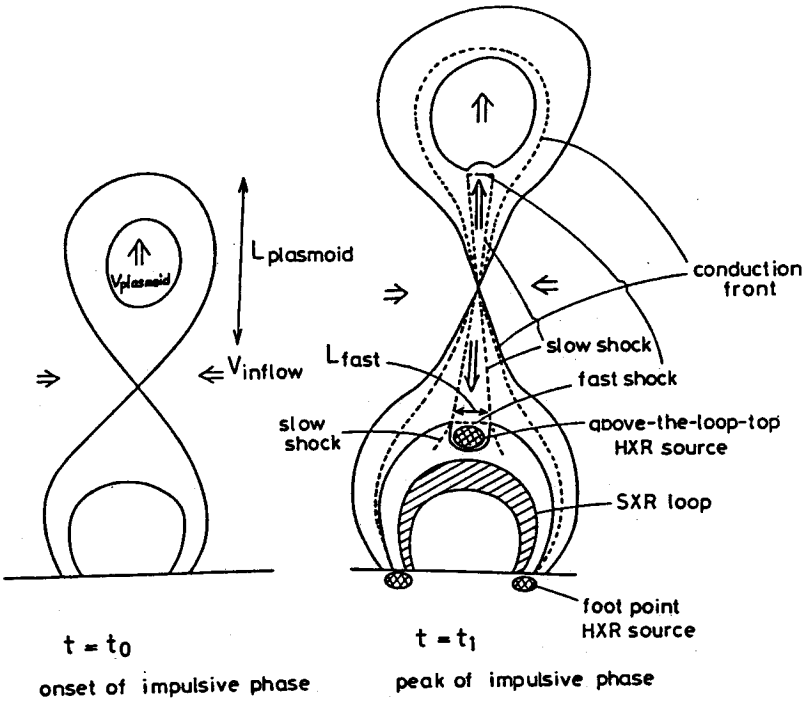

Figure 2. The *Plasmoid-Induced-Reconnection Model* for flares.

et al. 1996) or the sheared arcade case (e.g., Kusano et al. 1995, Magara et al. 1997), if there is a continuous driving motion to compress the current sheet or arcade, the following cycle is repeated: *current sheet or arcade* → *formation of plasmoids* → *ejection of plasmoids* → *recovery of the initial current sheet or arcade.* Note that although the evolution of the system is driven by external agents, the reconnection rate or the energy release rate is determined by the local condtions (i.e., anomalous resistivity and plasmoid ejection). The highly intermittent and recurrent behavior is the basic feature of this model.

We shall discuss the role of plasmoid ejections in more detail. Often people have argued that filament (a kind of plasmoid) ejection is the source of flare energy. In our model, however, the energy source is not in a filament (plasmoid) itself, but is stored in a volume surrounding the filament (plasmoid). The role of the plasmoid ejection is simply to trigger fast reconnection (i.e., fast inflow into an X-point). Ohyama and Shibata (1997a,b) observationally confirmed that the kinetic energy of an ejected plasmoid is much smaller than the total flare energy in the case of some typical flares.

Let us consider a current sheet with a plasmoid (magnetic island) inside it (Fig. 4). Apparently, *the plasmoid inhibits the reconnection.* Only after the plasmoid has been ejected out of the current sheet, will reconnection become possible. Once the reconnection has begun, the released energy helps to accelerate the plasmoid. If the plasmoid's speed increases, then the speed of inflow into the neutral point will also increase. Since the inflow speed determines the reconnection rate, this means that the ultimate origin

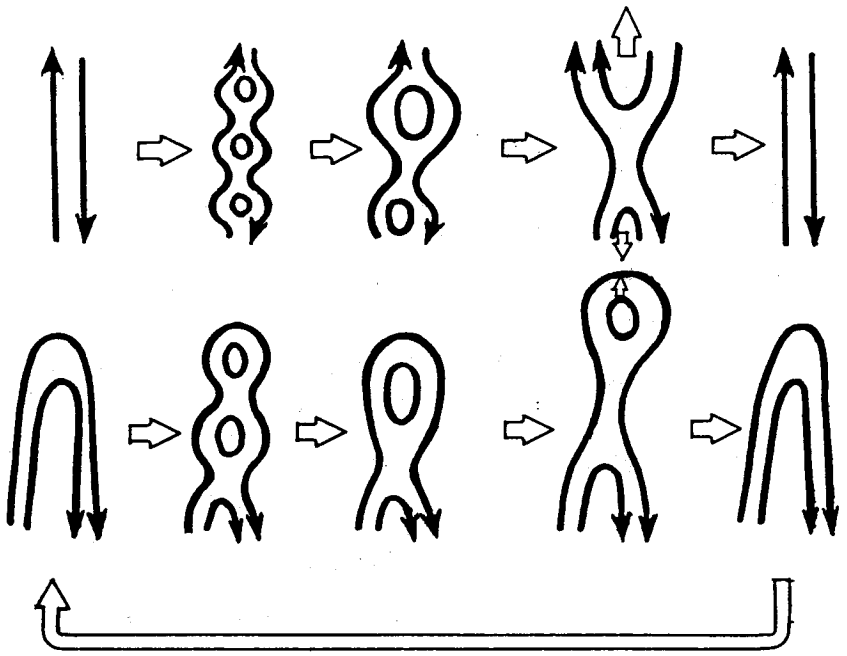

Figure 3. Recurrent behavior of plasmoid-induced-reconnection process, which naturally explains *homologous flares.*

of the fast reconnection is the fast ejection of the plasmoid.

This process can be understood as the collapse of a current sheet after the ejection of a plasmoid (Fig. 4). An important point is that the collapse itself is an ideal MHD process and the energy released during the collapse is non-negligible; indeed, it amounts to one-fourth of the magnetic energy stored in the original current sheet in the case of a simple model illustrated in Figure 4. In this case, once a large plasmoid has been ejected, at least one-fourth of the magnetic energy contained around the plasmoid will be released even if reconnection is inhibited after the ejection. Actually, the strong inflow due to the collapse induces fast impulsive reconnection, followed by a slow reconnection phase corresponding to the growth phase of a plasmoid, and vice versa, leading to intermittent fast reconnection (and plasmoid ejection). Each cycle (ejection of a plasmoid and triggered fast reconnection) may correspond to a different impulsive HXR/microwave peak in a flare with multiple peaks (Aschwanden et al. 1996).

Hence, as larger plasmoids are formed in the system, the stored magnetic energy becomes larger. Consequently, if a larger plasmoid is ejected, a larger energy release will occur.

2.2. APPLICATION TO IMPULSIVE FLARES

Magnetic reconnection theory predicts the existence of two oppositely directed high speed jets from the reconnection point with velocity at the

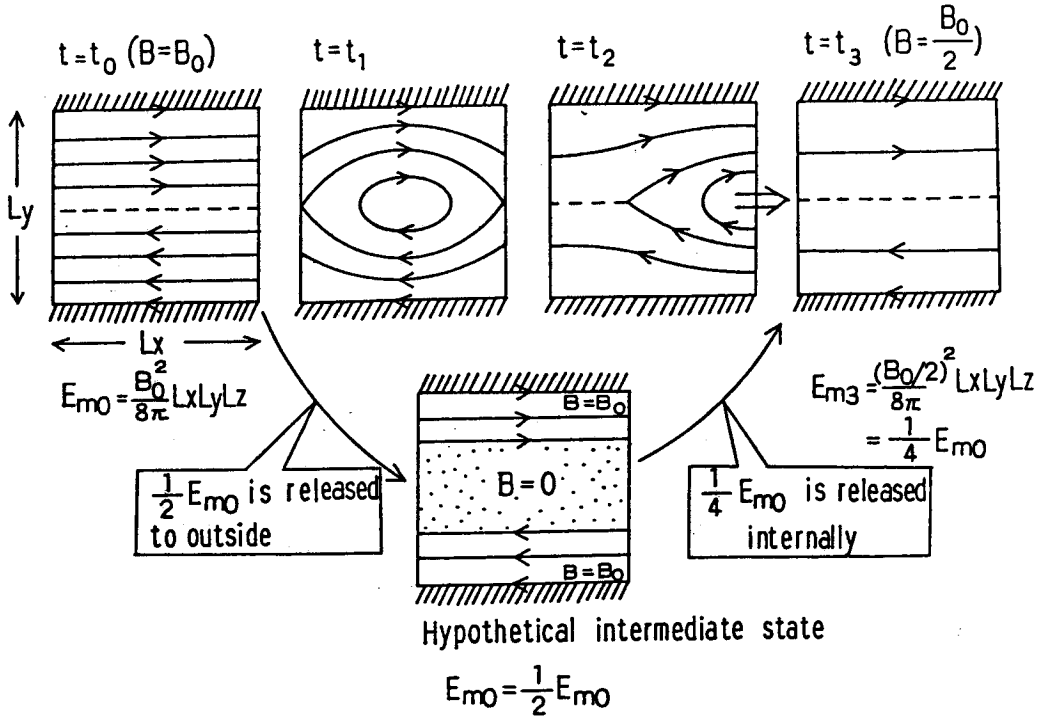

Figure 4. Detailed processes during the collapse of a current sheet accompanied by the ejection of a plasmoid. It is assumed here that half of the initial magnetic flux is reconnected to form a plasmoid ($t = t_1$). After the ejection of the plasmoid ($t = t_2$), the current sheet collapse occurs; i.e., the remaining magnetic flux expands to compress the current sheet. At the final stage ($t = t_3$), the magnetic field strength decreases to half of the initial value, and the magnetic energy in the box (E_{m3}) is one-forth of the initial magnetic energy ($E_{m3} = E_{m0}/4$, where E_{m0} is the initial magnetic energy contained in the box). This process and the effect of the collapse of the current sheet is more easily understood if we consider a hypothetical intermediate state between the ejection of the plasmoid and the collapse; i.e., a state in which half of the initial magnetic flux is removed out but the remaining flux has not yet expanded. After this hypothetical state, the remaining flux expands to fill the box. This process (i.e., the current sheet collapse) releases *one-forth of the initial magnetic energy.* It is interesting to note that this is an ideal MHD process. Hence even if the reconnection is inhibited after the ejection of the plasmoid, we can expect that one-forth of the initial magnetic energy is released by the collapse of the current sheet.

Alfven speed,

$$V_{jet} \sim V_A \simeq 2000\left(\frac{B}{100\mathrm{G}}\right)\left(\frac{n}{10^{10}\mathrm{cm}^{-3}}\right)^{-1/2}\mathrm{km/s}. \qquad (3)$$

The downward jet collides with the top of the SXR loop, producing an MHD fast shock. We consider that a very hot region heated by the fast shock corresponds to a loop-top impulsive HXR source. The temperature just behind the fast shock becomes

$$T_{fast} \sim mV_{jet}^2/(6k) \simeq 1 \times 10^8\ \mathrm{K}\left(\frac{B}{100\mathrm{G}}\right)^2\left(\frac{n}{10^{10}\mathrm{cm}^{-3}}\right)^{-1}, \qquad (4)$$

where m is the proton mass and k is the Boltzmann constant. This explains the observationally estimated temperature of the loop-top HXR source (Masuda 1994).

The extent of the fast shock, L_{fast} (see Fig. 2), is of order of

$$L_{fast} \sim \frac{V_{inflow}}{V_A} L_{plasmoid} \simeq M_A L_{plasmoid} \simeq 1000\mathrm{km}\left(\frac{M_A}{0.05}\right)\left(\frac{L_{plasmoid}}{2 \times 10^9\mathrm{cm}}\right). \quad (5)$$

The volume emission measure of the very hot region behind the fast shock becomes

$$EM_{fast} \sim n^2 {L_{fast}}^3 \simeq 10^{44}\mathrm{cm}^{-3}\left(\frac{n}{10^{10}\mathrm{cm}^{-3}}\right)^2\left(\frac{M_A}{0.05}\right)^3\left(\frac{L_{plasmoid}}{2 \times 10^9\mathrm{cm}}\right)^3. \quad (6)$$

Here, we assumed that the extent of the fast shock in the direction perpendicular to the plane of Figure 2 is comparable to that parallel to the plane. This value is roughly comparable to the actually observed emission measure of loop-top impulsive HXR sources, $10^{44} - 10^{46}$ cm^{-3} (Masuda 1994).

The time scale of the impulsive phase is determined from the duration of the strong inflow, which may be comparable to the travel time of the plasmoid across its size, i.e.,

$$t_{imp} \sim \frac{L_{plasmoid}}{V_{plasmoid}} \sim 20 t_A \left(\frac{M_A}{0.05}\right)^{-1}$$

$$\sim 200 \text{ sec} \left(\frac{M_A}{0.05}\right)^{-1}\left(\frac{B}{100\mathrm{G}}\right)^{-1}\left(\frac{n_e}{10^{10}\mathrm{cm}^{-3}}\right)^{1/2}\left(\frac{L_{plasmoid}}{2 \times 10^9\mathrm{cm}}\right), \quad (7)$$

where $t_A = L_{plasmoid}/V_A$. This is roughly consistent with the observed duration (1 – 3 min) of one impulsive peak. (The total duration of the impulsive phase ranges from 1 min to 10 min. Longer impulsive phases usually include multiple impulsive peaks.)

The magnetic energy stored around the current sheet and the plasmoid is suddenly released through reconnection into kinetic, thermal, and nonthermal energies after the plasmoid is ejected. The magnetic energy release rate at the current sheet (with the length of $L_{cs} \sim L_{plamoid} \simeq 2 \times 10^4$ km) is estimated to be

$$\frac{dE}{dt} = 2 \times L_{plasmoid}^2 B^2 V_{inflow}/4\pi$$

$$\sim 4 \times 10^{28} \text{ erg/s} \left(\frac{V_{inflow}}{100 \text{ km/s}}\right)\left(\frac{B}{100 \text{ G}}\right)^2\left(\frac{L_{plasmoid}}{2 \times 10^9 \text{ cm}}\right)^2. \quad (8)$$

This is comparable with the energy release rate during the impulisve phase, $4 - 100 \times 10^{27}$ erg/s, estimated from the footpoint HXR source (Masuda 1994), assuming the thick target model and the lower cutoff energy of nonthermal electrons as 20 keV.

Table I Application of Plasmoid-Induced-Reconnection Model to Various Flares

flare	B (G)	n (cm^{-3})	$L_{plasmoid}$ (cm)	T_{fast} (K)	EM_{fast} (cm^3)	t_{imp} (sec)	$\dot{E}$ (erg/s)
impulsive	100	10^{10}	2×10^9	10^8	10^{44}	200	10^{28}
LDE	30	$10^{9.5}$	4×10^9	$10^{7.5}$	10^{44}	700	2×10^{27}
giant arcade	10	10^9	6×10^9	10^7	$10^{43.5}$	1700	3×10^{26}
microflares	100	10^{10}	4×10^8	10^8	10^{42}	40	4×10^{26}

3. Application to LDE Flares, Giant Arcades, and Microflares

Observations show many common features in impulsive flares, LDE flares, giant arcades associated with filament eruptions or CMEs, and even microflares. For example, Shimojo, Yaji, and Shibata (1995) found an X-ray jet ejected from an M-class impulsive flare.

We can apply the above equations to LDE flares, giant arcades, and microflares. The results are summarized in Table I, where the magnetic field strength B is assumed to be comparable to the average photospheric field strength in the flare-occurring regions. These numbers are applicable to the impulsive phase or the rise phase. From this table, we predict that the loop-top HXR source in LDE flares has lower temperature ($\sim$ 30 MK) than that of impulsive flares, and its time scale is longer. We also predict that microflares have loop-top HXR source of temperatures similar to those of impulsive flares, although the emission measure of the source is much less and is not easily detected. We also expect it to be difficult to observe plasmoid ejections in microflares, because the plasmoids would collide and reconnect with ambient fields and disappear in a short time scale ($<$ 100 sec).

4. Discussion

Ground based observations suggest that emerging flux plays an important role in driving flares (e.g., Kurokawa 1987, Zhang et al 1997, Nishio et al. 1997, Hanaoka 1997). For example, a famous X-class impulsive flare, the 15 Nov 1992 flare (e.g., Sakao et al. 1992), was driven by a moving satellite spot (or emerging flux). Even the 21 Feb 1992 LDE flare (e.g.,

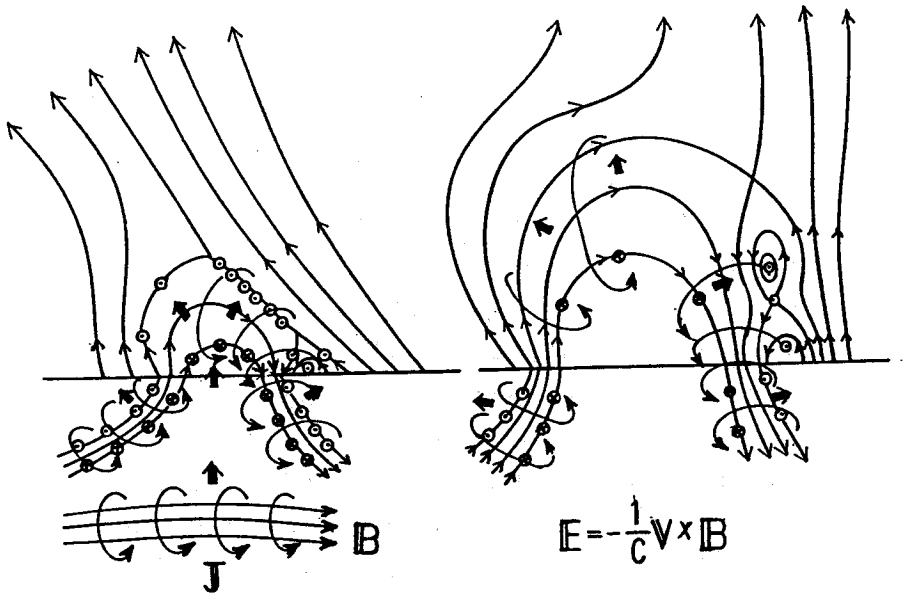

Figure 5. Current circuit and origin of electric field in a unified model (*plasmoid-induced-reconnection model*). This model unifies both the CSHKP model and the emerging flux model. Since the origin of electric field is emerging flux, this scheme may be called also the generalized emerging flux model.

Tsuneta 1996), and a homologous to it on 24 Feb 1992 (Morita et al. 1997) seem to be driven by growing flux (or emerging flux) (Zhang et al. 1997). Nevertheless, these flares clearly show filament or plasmoid ejections as well as the morphology predicted by the CSHKP model. Thus there is a need to unify the CSHKP and the emerging flux models. Such a unification is indeed possible in our *plasmoid-induced-reconnection model* as illustrated in Figure 5, in which it is shown that the driving electric field may originate from emerging flux.

The author would like to thank T. Yokoyama, K. Kusano, T. Hayashi, M. Ohyama, and S. Tsuneta for stimulating discussions.

References

Acshwanden, M. J., et al. 1996, ApJ, 464, 985.
Hanaoka, Y. 1997, in these proceedings.
Heyvaerts, J., Priest, E. R. and Rust, D. M. 1977, ApJ, 216, 123.
Karpen, J. T., Antiochos, S. K., and DeVore, C. R. 1995, ApJ, 450, 422.
Kitabata, H., Hayashi, T., Sato, T., et al. 1996, J. Phys. Soc. Japan, 65, 3208.
Kosugi, T., and Shibata, K. 1997, in Proc. Chapman Conference, Magnetic Storms, Geophysical Monograph 98, AGU, p. 21.

Kurokawa, H. 1987, Space Sci. Rev. 51, 49.
Kusano, K., Suzuki, Y., and Nishikawa, K. 1995, ApJ, 441, 942.
Lee, L. C., and Fu, Z. F. 1986, J. Geophys. Res., 91, 6807.
Magara, T., et al. 1996, ApJ, 466, 1054.
Magara, T., Shibata, K., Yokoyama, T. 1997, ApJ, in press.
Masuda, S. 1994, Ph. D. Thesis, U. Tokyo.
Masuda, S., et al. 1994, Nature, 371, 495.
Masuda, S., et al. 1995, PASJ, 47, 677.
Morita, S., et al. 1997, in these proceedings.
Nishio, M., et al. 1997, ApJ, in press.
Ohyama, M., and Shibata, K. 1997a, PASJ, 49, 249.
Ohyama, M., and Shibata, K. 1997b, ApJ, submitted.
Priest, E. R. 1982, Solar Magnetohydrodynamics, Reidel.
Sakao, T., et al. 1992, PASJ, 44, L83.
Shibata, K., Nozawa, S., and Matsumoto, R. 1992a, PASJ, 44 , 265.
Shibata, K., et al. 1992b, PASJ, 44, L173.
Shibata, K., et al. 1994, ApJ, 431, L51.
Shibata, K., et al. 1995, ApJ, 451, L83.
Shibata, K. 1996, Adv. Space Res., 17, (4/5)9.
Shibata, K. 1997, Proc. of Hitachi Solar Flare Workshop, T. Sakurai et al. (eds.) in press.
Shimizu, T. 1995, PASJ, 47, 251.
Shimojo, M., et al. 1996, PASJ, 48, 123.
Shimojo, M., Yaji, K., Shibata, K. 1995, ASJ fall meeting abstract (in Japanese).
Tsuneta, S., et al. 1992a, PASJ, 44, L63.
Tsuneta, S., et al. 1992b, PASJ, 44, L211.
Tsuneta, S. 1996, ApJ, 456, 840.
Tsuneta, S. 1997, ApJ, 483, 507.
Ugai, M. 1989, Phys. Fluids B, 1, 942.
Yokoyama, T., and Shibata, K. 1994, ApJ, 436, L197.
Yokoyama, T., and Shibata, K. 1995, Nature, 375, 42.
Yokoyama, T., and Shibata, K. 1996, PASJ, 48, 353.
Yokoyama, T., and Shibata, K. 1997, ApJ, 474, L61.
Yokoyama, T. 1997, in these proceedings.
Zhang, H. Q., et al. 1997, in these proceedings.
Watanabe, T. 1994, in Proc. Kofu Symposium, p. 99.